J. Microbiol. Biotechnol. (2006), **16**(6), 911–920

JOURNAL OF MICROBIOLOGY AND BIOTECHNOLOGY

Proteomic Analysis of Resting and Activated Human CD8$^+$ T Cells

KOO, JUNG-HUI[1], WOOK-JIN CHAE[2], JE-MIN CHOI[2], HYUNG-WOOK NAM[1], TOMOHIRO MORIO[3], YU-SAM KIM[1], YANG-SOO JANG[4], KWAN-YONG CHOI[5], JUNG-JIN YANG[6], AND SANG-KYOU LEE[2]*

[1]*Department of Biochemistry, Protein Network Research Center, Yonsei University, Seoul 120-749, Korea*
[2]*Department of Biotechnology, Yonsei University, Seoul 120-749, Korea*
[3]*Department of Pediatrics, Tokyo Medical and Dental University, School of Medicine, Tokyo 113-8519, Japan*
[4]*Cardiovascular Center, Yonsei University, Seoul 120-749, Korea*
[5]*Department of Life Science, Pohang University of Science and Technology, Kyungbuk 790-784, Korea*
[6]*School of Computer Science and Information Engineering, The Catholic University of Korea, Yeouido Post Office, P.O. Box 960, Seoul Korea*

Received: October 28, 2005
Accepted: December 24, 2005

Abstract CD8$^+$ T lymphocytes with the cytotoxic activity and capability to release various cytokines are the major players in immune responses against viral infection and cancer. To identify the proteins specific to resting or activated human CD8$^+$ T cells, human CD8$^+$ T cells were activated with anti-CD3+anti-CD28 mAb in the presence of IL-2. The solubilized proteins from resting and activated human CD8$^+$ T cells were separated by high-resolution two-dimensional polyacrylamide gel electrophoresis, and their proteomes were analyzed. Proteomic analysis of resting and activated T cells resulted in identification of 35 proteins with the altered expression. Mass spectrometry coupled with Profound and SWISS-PROT database analysis revealed that these identified proteins are to be functionally associated with cell proliferation, metabolic pathways, antigen presentation, and intracellular signal transduction pathways. We also identified six unknown proteins predicted from genomic DNA sequences specific to resting or activated CD8$^+$ T cells. Protein network studies and functional characterization of these novel proteins may provide new insight into the signaling transduction pathway of CD8$^+$ T cell activation.

Key words: Human CD8$^+$ T lymphocytes, two-dimensional electrophoresis (2-DE), matrix-assisted laser desorption - time of flight mass spectrometry (MALDI-TOF MS), T-cell activation

Cell-mediated immunity via CD8$^+$ T lymphocytes is important for the elimination of infectious pathogens and tumor cells. The encounter between CD8$^+$ T lymphocytes and antigen-presenting cells initiates T-cell receptor (TCR)-mediated and costimulatory signals to produce various kinds of surface and secretory effector molecules for the induction of immune response against infectious pathogens and cancer [29].

Although the TCR-mediated signaling is the major component for acquiring effector functions by CD8$^+$ T lymphocytes, the costimulatory signals via CD28 or ICOS are required for optimal production of effector cytokines or cytolytic molecules [1, 4, 24, 31]. As the dysfunction of immune responses in several pathological situations are frequently relevant with anergic or partially functional CD8$^+$ T lymphocytes, it is particularly important to understand the molecular mechanisms responsible for effector functions and the metabolic changes during antigenic stimulation [6, 19, 20]. Several experimental approaches including DNA microarray have been performed to explain the possible molecular mechanisms of effector functions of CD8$^+$ T lymphocytes by using the murine models with viral infection or human peripheral blood [8, 13, 15, 22, 23, 26, 27].

However, identification of the proteome specific to resting or activated human CD8$^+$ T lymphocytes using proteomic analysis has not yet been performed. In this study, human CD8$^+$ T lymphocytes were negatively purified from human peripheral blood leukocytes (PBL) via Ab-mediated magnetic separation, and the proteomic analysis was performed with resting or activated human CD8$^+$ T cells with anti-CD3 and anti-CD28 mAb. The protein spots specific to resting or activated CD8$^+$ T cells were characterized by two-dimensional electrophoresis and MALDI-TOF MS analysis.

*Corresponding author
Phone: 82-2-2123-2889; Fax: 82-2-362-7265;
E-mail: sjrlee@yonsei.ac.kr

Materials and Methods

Purification of $CD8^+$ T Lymphocytes

Leukocyte-rich buffy coats were prepared from healthy blood donors, and mononuclear cells were freshly purified. Briefly, an equal volume of PBS and buffy coats were mixed, layered on Histopaque 1077 (Sigma, St. Louis, MO, U.S.A.), and then centrifuged for 30 min. White blood cells were recovered and washed three times with the buffer (2% Bovine serum albumin and 2 mM EDTA in ice-cold PBS), and $CD8^+$ T lymphocytes were negatively purified by MACS (Miltenyi Biotech, Gladbach, Germany) using a $CD8^+$ T-cell isolation Kit II (Miltenyi Biotech). The purified cells were incubated with FITC-conjugated human anti-CD8 antibody (Miltenyi Biotech) and PE-conjugated human anti-CD3 antibody (Dako, Glostrup, Denmark) for examining the cell purity. The average purity of the purified $CD8^+$ T cells was 98.5%.

Flow Cytometric Analysis of the Activated Human $CD8^+$ T Cell

Human $CD8^+$ T cells (1.0×10^7) were incubated on ice with 1 μg/ml of anti-CD28 (BD Pharmingen, San Diego, CA, U.S.A.) for 15 min, washed with ice-cold PBS, and subsequently stimulated in the flasks coated with 5 μg/ml of anti-CD3 mAb in the presence of 100 U/ml of IL-2. Cells were maintained with RPMI 1640 (Biowhittaker, Walkersville, MD, U.S.A.) culture medium containing 10% human serum (Biowhittaker), 1% sodium pyruvate (Biowhittaker), 0.2 U/ml insulin (Sigma),1 mM oxalacetic acid (Sigma), 2 mM L-glutamine (Biowhittaker), and 50 μg/ml kanamycin (Sigma). After 96 h of activation, cells were harvested, washed with PBS three times, and snap frozen in liquid nitrogen until further analysis. Cells for flow cytometric analysis were stained with FITC-conjugated anti-human CD45RA, CD95, CD25, and PE-conjugated anti-human CD27, CD152, CD28, and CCR7 (BD Pharmingen) and analyzed by FACSCalibur (Becton-Dickinson) using CellQuest software.

Sample Preparation, Isoelectricfocusing (IEF), and Two-Dimensional Electrophoresis (2-DE)

Cells were lysed in lysis buffer, containing 40 mM Tris-base, 2% NP-40, 4% CHAPS, 200 mM DTT, 5 mM $MgCl_2$, and protease inhibitor cocktail (Roche, Mannheim, Germany), for 30 min at 37°C with shaking. The insoluble material was cleared by ultracentrifugation at 48,000 rpm for 30 min at 15°C, and the protein concentration was determined by the Bradford assay. Three-hundred μl of solubilizing buffer [7 M urea, 2 M thiourea, 2% NP-40, 0.5% IPG-buffer 3–10 NL, 2 mM tributyl phosphine (TBP), 0.002% bromophenol blue] were added to the cell lysate and incubated at room temperature for 30 min. After centrifugation at 14,000 rpm and 4°C for 15 min, the sample mixture was applied to the Immobiline DryStrips (pH 3–10 nonlinear, 18 cm; Amersham Pharmacia Biotech, Uppsala, Sweden) with the in-gel sample application method for 24 h at room temperature. IEF was carried out with 50 V for 10 h, 100 V for 1 h, 300 V for 1 h, 600 V for 1 h, and 8,000 V for 10 h to reach the total of 90–106 kVh. Then, the DryStrips were equilibrated with equilibration solution [6 M urea, 2% SDS, 1.875 M Tris-HCl (pH 8.8), 20% glycerol, 2.5% acryl amide, and 5 mM TBP] for 15 min with gentle shaking. The gel used in this study was a gradient formed from 9–16% acrylamide (23×20×0.1 cm). Electrophoresis was performed in the IsoDalt (Hoeffer, San Francisco, CA, U.S.A.) until the tracking dye reached the anodic end of the gel.

Silver Nitrate Staining, In-Gel Digestion, and Peptide Extraction

The analytical gel was stained according to the previous protocol for silver staining by Jun *et al.* [30]. The gel was fixed twice in 40% methanol and 10% acetic acid for 15 min and sensitized with 30 min of incubation in the solution containing 30% methanol, 5% sodium thiosulfate, and 6.8% (w/v) sodium acetate and rinsed for 5 min with distilled water three times. After incubation in 2.5% silver nitrate solution for 20 min, the gel was rinsed twice with distilled water for 1 min and then developed in 2.5% (w/v) sodium carbonate and 0.04% (v/v) formaldehyde. The developing procedure was terminated by washing with 1.46% EDTA for 10 min and then washed with distilled water three times. Each silver-stained protein spot was excised and destained in 120 μl of 1:1 mixing solution of 30 mM potassium perricyanide and 100 mM sodium thiosulfate with vortexing, and washed three times for 5 min with distilled water. The spots were rinsed three times with a solution (50% acetonitrile/25 mM NH_4HCO_3) for 10 min with vortexing and dried for 1 h. Enzymatic digestion was performed with 10 μl of 0.01 μg/μl trypsin in 25 mM ammonium bicarbonate, (pH 8.5) at 37°C for 16 h. To extract digested peptides, 10 μl of 0.1% trifluoroacetic acid (v/v; TFA) in 50% v/v acetonitrile were added to each tube and sonicated for 30 min three times in an ultrasonic water bath (Branson Ultrasonic Corp, Danbury, CT, U.S.A.). Finally, the extracted peptides were dried in a speed vacuum centrifuge.

MALDI-TOF MS Analysis of Tryptic Peptides

Peptide mass fingerprinting analysis was performed on a PerSeptive Biosystems Voyager-DE STR MALDI-TOF-MS (Applied Biosystems, Framingham, MA, U.S.A.) in reflectron mode. The extracted peptide (0.5–1 μl) was dispensed onto a MALDI sample plate along with 0.5–1 μl of matrix solution consisting of 10 mg/ml α-cyano-4-hydroxycinnamic acid, 0.1% TFA, and 50% acetonitrile. The sample was dried under the ambient condition. Internal mass calibration was performed with trypsin autodigestion

Table 1. Identification of the landmark proteins from resting and activated $CD8^+$ T lymphocytes.

Spot No.	Protein name	Accession No.	Mr/pI	Sequence coverage (%)	Amino acid sequences
L1	Lactate dehydrogenase B	NP_002291	36615/5.71	12%	LIAPVAEEEATVPNNK IVVVTAGVR FIIPQIVK GLTSVINQK
L2	2-Phosphopyruvate-hydratase alpha-enolase	CAA59331	47079/7.01	24%	GNPTVEVDLFTSK AAVPSGASTGIYEALELR AVEHINK TIAPALVSK LNVTEQEK DATNVGDEGGFAPNILENK EGLELLK YISPDQLADLYK YNQLLR IEEELGSK
L3	p64 CLCP	CAA61020	23528/5.12	22%	GVTFNVTTVDTK FSAYIK NSNPALNDNLEK GFTIPEAFR YLSNAYAR
L4	Folate-binding protein	AAA74896	26264/8.30	6%	NACCSTNTSQEAHK
L5	Triosephosphate isomerase	P00939	26609/4.10	35%	HVFGESDELIGQK VVFEQTK VVLAYEPVWAIGTGK TATPQQAQEVHEK SNVSDAVAQSTR ELASQPDVDGFLVGGASLKPEFVDIINAK
L6	Proteasome activator subunit 1 isoform 1	NP_006254	28705/5.78	13%	IVVLLQR IEDGNNFGVAVQEK NAYAVLYDIILK
L7	Cofilin 1 (non-muscle)	NP_005498	18491/8.22	36%	NIILEEGK EILVGDVGQTVDDPYATFVK YALYDATYETK MIYASSK LGGSAVISLEGKPL
L8	Heat-shock 60 kDa protein 1 (chaperonin)	NP_002147	61016/5.70	10%	LVQDVANNTNEEAGDGTTTATVLAR GANPVEIR VGLQVVAVK LSDGVAVLK VTDALNATR
L9	Thioredoxin-like; PKC-interacting cousin of thioredoxin	NP_006532	37466/5.25	5%	ELPQVSFVK

The identified nine spots (L1–L9) are from Coomassie brilliant blue G250 stained 2-DE gels in both resting and activated $CD8^+$ T cells and analyzed by using nano-LC/MS/MS. Database searches were performed with an NCBI nonredundant database using the MASCOT software package.

products, so that an average of 100–150 spectra for each sample was acquired in the delayed extraction and reflection mode [7].

Nano LC/MS/MS Analysis and Database Search

To establish the landmark proteins in 2-DE analysis, we identified 9 spots from Coomassie brilliant blue G250 stained gels in both resting and activated $CD8^+$ T cells, and analyzed them using nano-LC/MS/MS (Table 1). Briefly, 5 μl of a sample was loaded onto precolumn Zorbax resin (Agilent, Palo Alto, U.S.A.; 2 cm×200 μm I.D.) and washed with the loading solvent (H_2O/0.1% formic acid; flow rate: 20 nl/min) for 10 min to remove salts and denaturing reagents by the Switchos micropump. The sample in the

trapping column was eluted to the analytical column for separation by an ultimate nano pump, and the column eluant was directly coupled to the QSTAR quadrupole orthogonal TOF mass spectrometer (Applied Biosystems, Foster City, U.S.A.). The LC-MS runs on the QSTAR instrument were acquired in "Information Dependent Acquisition" mode (advanced IDA). Database searches were performed with an NCBI (National Center for Biotechnology Information) nonredundant database using the MASCOT software package (Matrix Sciences, London, U.K.).

Results and Discussion

Purification, Activation, and Phenotypic Characterization of Human CD8$^+$ T Lymphocytes

Cell-mediated immune responses to successfully eliminate viral pathogens and tumors require the differentiation of naïve CD8$^+$ T lymphocytes into effector ones. Along with

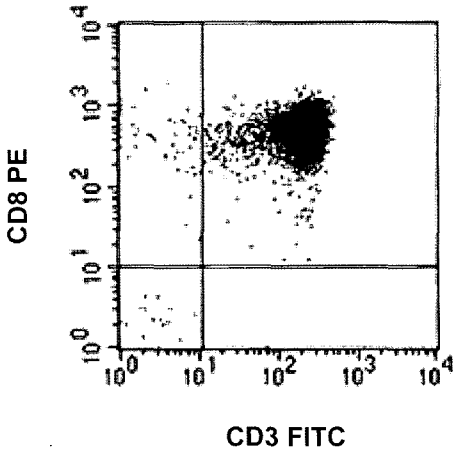

Fig. 1. Purification of human CD8$^+$ T lymphocytes.
Cells were purified using a biotin-conjugated monoclonal antibody cocktail and anti-biotin microbeads. The purified cells were analyzed for surface expression of TCR and CD8 by flow cytometry using PE-anti-human CD3 and FITC-anti-human CD8 antibodies.

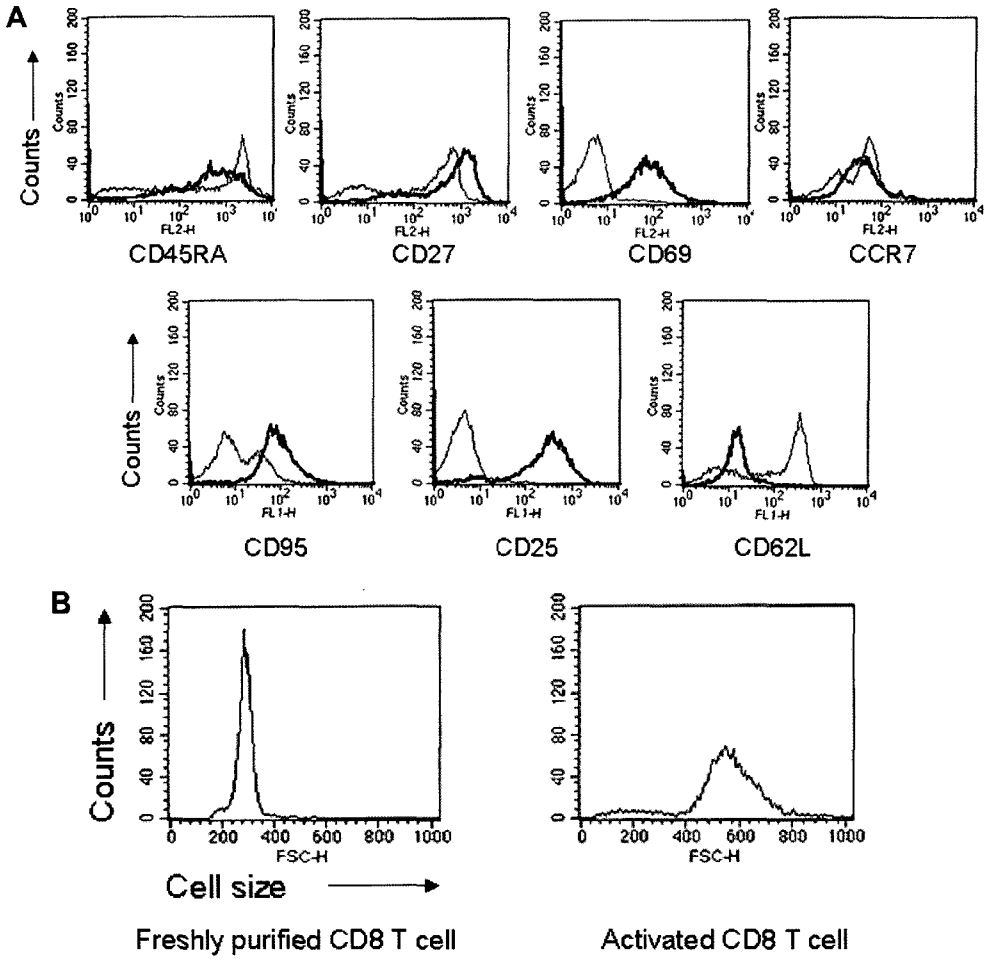

Fig. 2. Flow cytometry analysis of the purified and activated human CD8$^+$ T cells.
A. Cells were stimulated for 96 h with anti-CD3 and anti-CD28 antibodies in the presence of IL-2. After activation, cells were harvested and analyzed for various surface antigens by flow cytometry. Thin line: freshly purified resting CD8$^+$ T cells; thick line: activated CD8$^+$ T cells. **B.** Freshly isolated resting (left graph) and activated (right graph) CD8$^+$ T cells were analyzed for cell size. These are the representatives of six independent analyses.

these functional changes, the activated $CD8^+$ T cells are expected to undergo *de novo* synthesis or modification of proteins involved in cellular metabolism, migration, and intracellular signal transduction pathways.

PBMCs (9.3×10^8 cells) were used to obtain 8.4×10^6 of human $CD8^+$ T lymphocytes with more than 98% purity (Fig. 1). These $CD8^+$ T cells were purified by negative selection to eliminate the unwanted populations. The viability of the purified cells was over 98% when measured by Trypan Blue exclusion (data not shown). The purified total $CD8^+$ T lymphocytes were stimulated with flask-coated anti-CD3 antibody and anti-CD28 antibody in the presence of 100 U/ml IL-2 for 96 h to activate functional $CD8^+$ T cells. To examine the level of T-cell activation, these cells were harvested, and activation-dependent surface antigens were analyzed by flow cytometry. Analysis of activation-induced cell surface antigens on T cells such as CD69 and CD25 (IL-2 receptor alpha chain) clearly showed that the harvested cells were fully activated effector $CD8^+$ T cells. The expression profiles of CCR7 and CD95 indicated that these effector $CD8^+$ T cells were homogenous for their expression upon antigenic challenge, whereas these surface markers were expressed in comparatively low level before stimulation. The expression of CD28 or CD27 on $CD8^+$ T cells were not largely affected by TCR stimulation, although their overall expression level was slightly upregulated (Fig. 2A). The marked downregulation of lymphocyte homing receptor (CD62L) strongly suggested that these cells were differentiated into functional effector cells, so that their capability to enter HEV (high endothelial venule) was decreased, similar to naïve T cells. The cell size was increased with the changes of surface antigens, reflecting that the active metabolic changes occurred (Fig. 2B). Collectively, these results demonstrated that the $CD8^+$ T lymphocytes became fully activated by the stimulation of the TCR complex.

Two-Dimensional Eletrophoresis and Characterization of Differential Protein Spots Specific to Resting or Activated T Cells

To identify the activation-induced proteome of human $CD8^+$ lymphocytes with phenotypic activation profiles, the proteins were prepared from resting or activated $CD8^+$ T lymphocytes, and their proteomes were analyzed through 2-DE. After image acquisition from silver-stained gels, the protein spots were analyzed by Melanie 3.0 software to separate the specific protein spots from the nonspecific ones. Consistent with the phenotypic changes shown in flow cytometric analysis, about 400 more protein spots were detected from activated $CD8^+$ T cells between pH gradient of 3 and 10 (Fig. 3).

The molecular size of the extracted peptide from the differential protein spots in the silver-stained 2-DE gels was measured by MALDI-TOF-MS analysis and subsequently matched with the Profound and SWISS-PROT databases. The identity of proteins was searched in the SWISS-PROT and NCBI nonredundant databases using ProFound (The Rockefeller University Edition, Version 4.10.5). All mass searches were performed in the mass range between 6 kDa and 200 Da of *Homo sapiens* sequences. The search parameters were set for allowing the modification of cysteine by acrylamide. The criteria for the positive

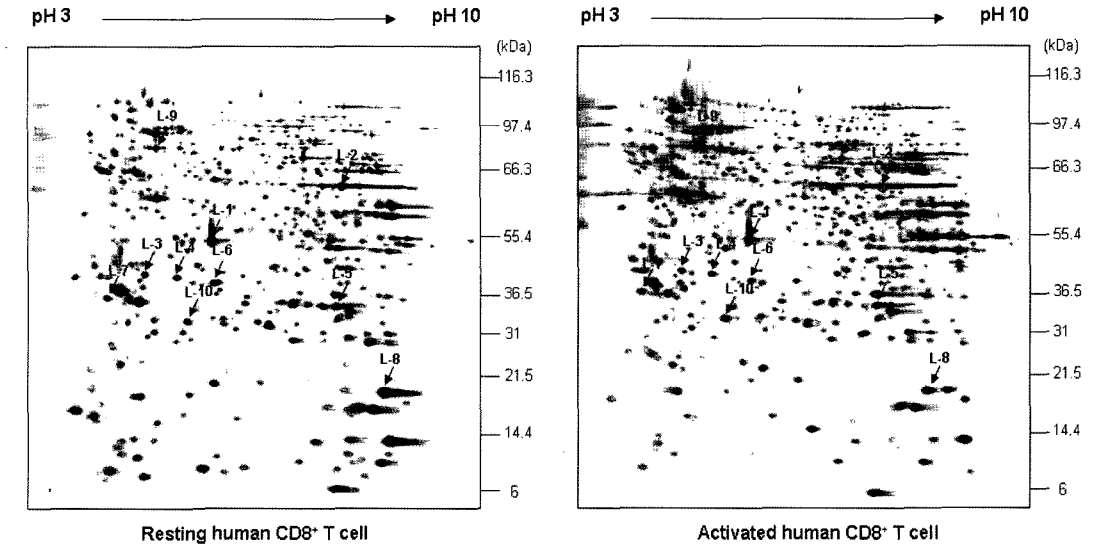

Fig. 3. 2-DE gel map derived from freshly isolated resting and activated human $CD8^+$ T cells.
Protein (100 μg) was applied to pH 3–10 nonlinear IPG strips (18 cm), with 9–16% gradient vertical SDS-PAGE as the second dimension. The gel was visualized by silver nitrate staining. The nine landmark proteins numbered L1–L9 correspond to their listings in Table 1. The results are the representative of seven experiments.

identification of proteins were as follows; (i) at least four matching peptide masses, (ii) 50 ppm or better mass accuracy, and (iii) molecular weight and pI of the identified protein should match the estimated value obtained from image analysis.

Among 400 spots, 56 proteins were chosen that showed more than three-fold differences in expression between resting and activated $CD8^+$ T cells, and the identity of 35 protein spots was revealed by Profound and MS-fit database search (Table 2). Among them, 21 spots appeared or were upregulated, and 14 spots disappeared or were downregulated upon TCR stimulation.

Since T-cell activation accompanies cell proliferation, it was of interest to identify the cell-cycle-regulating proteins from the identified protein spots. As shown in Table 2 and Fig. 4, we found the increased expression of proliferating cell nuclear antigen (PCNA) (S25-u), which has been previously known to be expressed upon stimulation [10]. Furthermore,

Table 2. Proteins differentially expressed in resting and activated human $CD8^+$ T lymphocytes.

Spot No.	Protein name	Accession No.	Mr/pI	Sequence coverage (%)
S7-a	dUTP pyrophosphatase	NP_001939	17.94/62	43%
S8-a	Cell division control-related protein 2	NP_536341	53.59/5.9	18%
S9-u	Fatty acid binding protein 5 (psoriasis-associated)	NP_001435	15.57/6.6	53%
S24-u	Proteasome (prosome, macropain) subunit, beta type, 7	AAH17116	29.62/8	13%
S25-u	Proliferating cell nuclear antigen; cyclin; DNA polymerase delta auxiliary protein	NP_002583	29.18/4.6	46%
S26-u	Cytosolic inorganic pyrophosphatase	AAD24964	32.39/5.4	37%
S30-a	Chain D, complex of Ran with Importin beta	1IBR_D	52.34/4.6	13%
S31-u	JUAA0002	BAA07652	59.2/5.8	24%
S33-u	T-Cell FK506-binding protein	NP_002005	52.14/5.3	41%
S34-u	Mitochondrial matrix processing protease, alpha subunit	NP_055975	58.87/6.4	16%
S37-u	HLA-B-1516	AAA18249	40.83/6	31%
S38-u	Alkaline phosphatase precursor	AAC97139	58.3/5.8	10%
S39-a	Adenosine deaminase	CAA26130	35.4/5.6	25%
S45-u	Tryptophanyl-tRNA synthetase	P23381	53.57/5.8	36%
S52-a	AF454057_1 SE2-5LT1 protein	AAN75697	90.03/6.3	13%
S53-a	Chaperonin-containing TCP1	NP_005989	61.1/6.1	27%
S63-u	Integrin, beta-like 1 (with EGF-like repeat domains)	NP_004782	59.59/5.4	12%
S73-a	Unnamed protein product	BAA91706	56.39/8.9	21%
S79-u	Ran-specific GTPase-activating protein	S40475	23.65/5.2	29%
S80-u	C Chain C, crystal structure of recombinant human fibrinogen fragment D	1LT9_C	35.59/5.9	12%
S83-a	Unnamed protein product	BAA91700	84.52/5	12%
R1-a	Unnamed protein product	BAC03847	38.85/4.9	12%
R10-u	Chain A, crystal structure of the Tpr1-domain of Hop in complex with a Hsc70-peptide	1ELW_A	13.55/6.3	52%
R11-a	Hypothetical protein XP_297995	XP_297995	11.18/5	56%
R14-a	TAR RNA binding protein 1 isoform b	NP_599151	11.9/6.8	49%
R18-u	Macrophage migration inhibitory factor (glycosylation-inhibiting factor)	NP_002406	12.67/7.9	45%
R42-a	Chromobox homolog 4	NP_003646	61.57/9.6	16%
R65/a	RP3	CAA72060	22.30/9.57	53%
R78-u	Unnamed protein product	BAA91262	14.26/4.8	35%
R84-u	Moesin	NP_002435	67.94/6.1	25%
R85-u	Moesin/anaplastic lymphoma kinase fusion protein	AAK71522	62.07/7.7	23%
R88-u	Proacrosin binding protein sp32 precursor	NP_115878	62.76/5.1	11%
R91-u	Aldo-keto reductase family 1	AAH05387	36.3/6.8	54%
R93-u	Cell division control-related protein 2	NP_536341	53.59/5.9	17%
R99-u	Unnamed protein product	BAB55196	39.79/5.2	18%

Protein identification was carried out by peptide mapping using MALDI-TOF followed by searches of SWISS-PROT and NCBI nonredundant databases using ProFound. All mass searches were performed in the mass range between 6 kDa and 200 kDa of *Homo sapiens* sequences.
S, stimulated status; R, resting status; a, appeared; u, upregulated.

cell division control-related protein 2 (S8-a), Ran-specific GTPase-activating protein (S79-u), and complex of Ran/Importin Beta (S30-a) were upregulated by TCR stimulation. In contrast to these, chromobox 4 (R42-u) was downregulated upon TCR stimulation (Fig. 4). Interestingly, chromobox 4 has been known to regulate the gene expression in many loci of chromosomes by repressing the gene transcription and replication by its binding to chromosomes [5, 14, 21]. Since chromobox 4 is a member of the polycomb group family of proteins and recruits gene-silencing factors by

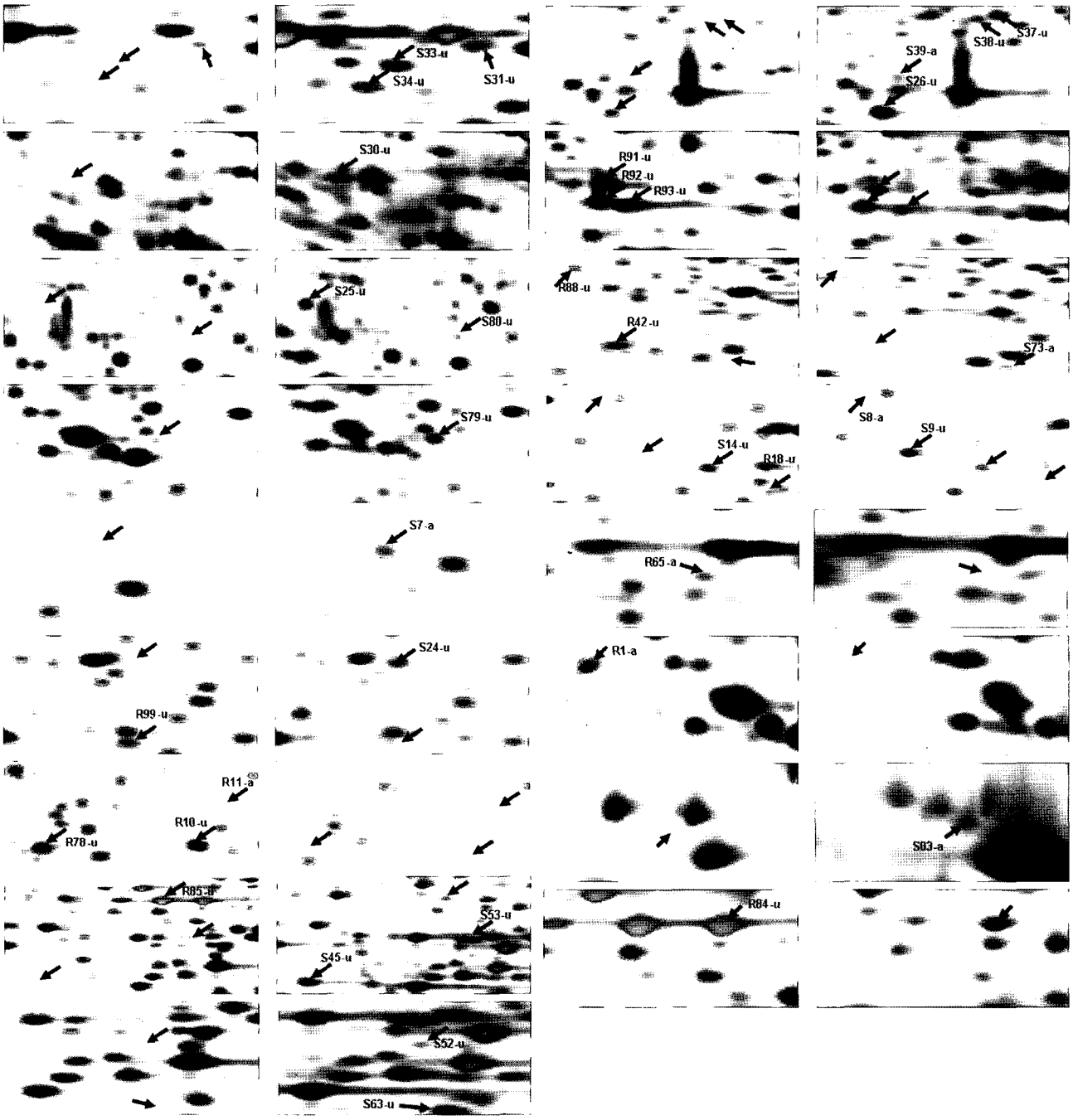

Fig. 4. Changes in protein expression between resting and activated human CD8+ T cells.
High magnification views of the differentially expressed regions of the gels in Fig. 3 are shown. The differentially expressed proteins whose expression level was more than three-fold increased in resting human CD8+ T cells (left panels), compared with activated human CD8+ T cells (right panels), were selected for MALDI-TOF MS analysis. The expression level was determined by the relative spot volume of the proteins compared with total amount of protein in the gel. The number of each protein spot corresponds to its listing in Table. 2. Data analysis was performed using Melanie 3.0 software. S, stimulated; R, freshly isolated resting; a, appeared; u, upregulated.

binding to PRE (polycomb responsive element) [9, 28], our results suggest that the TCR stimulation triggers downregulation of the gene silencing proteins and promotes upregulation of proteins involved in proliferation of human $CD8^+$ T cells.

Concomitant with these changes, a wide range of metabolic changes was observed. The expression of cytosolic inorganic pyrophosphatase (S26-u), dUTP pyrophosphatase (S7-a), adenosine deaminase (ADA) (S39-a), lipid metabolism related protein fatty acid binding protein 5 (psoriasis-associated) (S9-u), tryptophanyl-tRNA synthetase (S45-u), and mitochondrial matrix processing protease alpha subunit (S34-u) were upregulated (Table 2, Fig. 4).

Fatty acid binding protein 5 (FABP), a small and highly conserved cytoplasmic protein, which plays a role in fatty acid uptake and transport by binding to long-chain fatty acid, was also upregulated [11]. As an increase of this protein was also observed in epidermal cells and keratinocytes, its functions for $CD8^+$ T lymphocytes activation and proliferation remain to be addressed. One possible explanation for this upregulation may come from a recent study that epidermal fatty acid binding protein colocalizes with psoriasin in the cytoplasm, forming focal adhesion-like structures with alpha-actinin and paxillin in response to calcium challenge [18].

The upregulation of adenosine deaminase was well correlated with the increased expression of IL-2 receptor alpha chain following TCR stimulation, since this enzyme has been reported to prevent the immunosuppressive effect of adenosine in activated T lymphocytes [2]. It could be speculated that this ADA upregulation could sustain the activation status of $CD8^+$ T cell upon stimulation, and promote cell survival by preventing the accumulation of potential toxic metabolites such as dAMP, dADP, and dATP.

The expression of the human interferon-inducible tryptophanyl tRNA synthetase gene was increased upon phorbol 12-myristate 13-acetate (PMA) stimulation in HeLa and HEK 293 cells [32], and upregulated by IFN-gamma [17]. This may indicate that tryptophan metabolism is actively regulated by antigenic challenge to build up important proteins for immunological function.

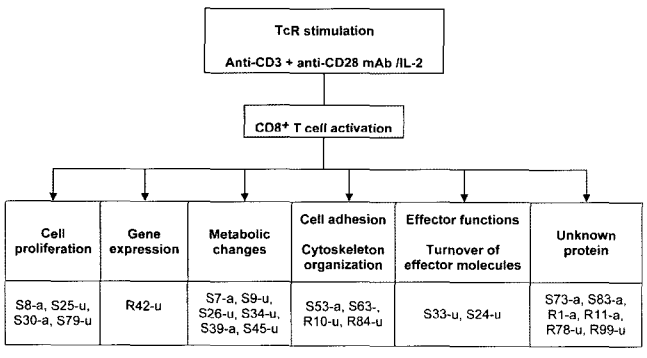

Fig. 5. Functional classification of the identified proteins.

We also found increased expression of molecules involved in cell adhesion and cytoskeletal organization such as chaperonin containing TCP1 (S53-a), integrin, beta-like 1 protein (S63-u), and decreased expression of the Tpr1 domain of Hop in complex with a Hsc-70 (R10-u) and moesin (R84-u). These proteins are important for activation-induced morphology changes and movement of effector molecules in T cells, and the migration of effector T cells to the target site, supporting the recent study on downregulation of moesin for enhancing the contact between T cells and antigen-presenting cell [3].

T-cell FK506-binding protein (S33-u) and proteasome subunit beta type 7 (S24-u), which are known to be essential for effector functions of $CD8^+$ T cells and turnover of effector molecules, were upregulated by TCR stimulation. Previous studies have shown that the proteasome subunit beta type 7 is upregulated by interferon-γ [9] and increased expression of T-cell FK506-binding protein upon antigenic challenge was reported previously [16, 25]. A recent report suggesting the role of T-cell FK506-binding protein in glucocorticoid receptor (GITR)-mediated signaling substantiates that the upregulation of T-cell FKBP is highly dependent on T-cell activation through TCR, especially in association with hsp90 and hsp70.

Several proteins corresponding to predictions from genomic DNA sequences that were upregulated in activated (S73-a, S83-a) or resting $CD8^+$ T lymphocytes (R1-a, R11-a, R78-u, R99-u) were identified, but their functions have not previously been characterized. Functional analysis of these proteins in the activation, proliferation, and effector functions of $CD8^+$ T lymphocytes is being undertaken, which can contribute to further understanding of CTL-mediated immune responses.

In this study, we were prompted to perform the proteomic analysis with resting and TCR-stimulated human $CD8^+$ T lymphocytes to identify differential proteomes, so that we can shed some light on various perspectives on human effector $CD8^+$ T-cell biology. Although a few approaches have been tried in terms of microarray, our study is the first report on the proteome of human effector $CD8^+$ T cells with antigenic stimulation.

Acknowledgments

We are thankful to Prof. Norio Shimizu and Prof. Alfred Bothwell for the comments on the manuscript, and all members of the Immune Cell Engineering Laboratory, Department of Biotechnology, Yonsei University for their spiritual help. This work was supported in part by research grants from the Korea Institute of Industrial Technology Evaluation and Planning (M1-0310-40-0000), Korea Health Industry Development Institute (0412-DB00-0101-0011), Korea Science and Engineering Foundation (2005-00117),

Korea Rural Economic Institute (204081-3), and Protein Network Research Center.

REFERENCES

1. Alegre, M.-L., K. A. Frauwirth, and C. B. Thompson. 2001. T-Cell regulation by CD28 and CTLA-4. *Nat. Rev. Immunol.* **1:** 220–228.
2. Butler, J. J., J. S. Mader, C. L. Watson, H. Zhang, J. Blay, and D. W. Hoskin. 2003. Adenosine inhibits activation-induced T cell expression of CD2 and CD28 costimulatory molecules: Role of interleukin-2 and cyclic AMP signaling pathways. *J. Cell. Biochem.* **89:** 975–991.
3. Faure, S., L. I. Salazar-Fontana, M. Semichon, V. L. Tybulewicz, G. Bismuth, A. Trautmann, R. N. Germain, and J. Delon. 2004. ERM proteins regulate cytoskeleton relaxation promoting T cell-APC conjugation. *Nat. Immunol.* **5:** 272–279.
4. Hutloff, A., A. M. Dittrich, K. C. Beier, B. Eljaschewitsch, R. Kraft, I. Anagnostopouls, and R. A. Kroczek. 1999. ICOS is an inducible T-cell co-stimulator structurally and functionally related to CD28. *Nature* **397:** 263–266.
5. Kagey, M. H., T. A. Melhuish, and D. Wotton. 2003. The polycomb protein Pc2 is a SUMO E3. *Cell* **113:** 127–137.
6. Kang, K. Y., C. H. Choi, J. Y. Oh, H. Kim, G. R. Kweon, and J. C. Lee. 2005. Chloramphenicol arrests transition of cell cycle and induces apoptotic cell death in myelogenous leukemia cells. *J. Microbiol. Biotechnol.* **15:** 913–918.
7. Kim, M. J., H. J. Chung, S. M. Park, S. G. Park, D. K. Chung, M. S. Yang, and D. H. Kim. 2004. Matrix-assisted laser desorption/ionization time-of-flight (MALDI-TOF)-based cloning of enolase, ENO1, from *Cryphonectria parasitica*. *J. Microbiol. Biotechnol.* **14:** 620–627.
8. Lee, H. Y., J. H. Park, S. H. Seok, S. A. Cho, M. W. Baek, D. J. Kim, Y. H. Lee, and J. H. Park. 2004. Dietary intake of various lactic acid bacteria suppresses type 2 helper T cell production in antigen-primed mice splenocyte. *J. Microbiol. Biotechnol.* **14:** 167–170.
9. Levine, S. S., A. Weiss, H. Erdjument-Bromage, Z. Shao, P. Tempst, and R. E. Kinston. 2002. The core of the polycomb repressive complex is compositionally and functionally conserved in flies and humans. *Mol. Cell. Biol.* **22:** 6070–6078.
10. Liu, K., M. Catalfamo, Y. Li, P. A. Henkart, and N.-P. Weng. 2002. IL-15 mimics T cell receptor crosslinking in the induction of cellular proliferation, gene expression, and cytotoxicity in CD8$^+$ memory T cells. *Proc. Natl. Acad. Sci. USA* **99:** 6192–6197.
11. Madsen, P., H. H. Rasmussen, H. Leffers, B. Honore, and J. E. Celis. 1992. Molecular cloning and expression of a novel keratinocyte protein (psoriasis-associated fatty acid-binding protein [PA-FABP]) that is highly up-regulated in psoriatic skin and that shares similarity to fatty acid-binding proteins. *J. Invest. Dermatol.* **99:** 299–305.
12. Nandi, D., H. Jiang, and J. J. Monaco. 1996. Identification of MECL-1 (LMP10) as the third IFN-γ-inducible proteasome subunit. *J. Immunol.* **156:** 2361–2364.
13. Nilges, K., H. Hohn, H. Pilch, C. Neukirch, K. Freitag, P. J. Talbot, and M. J. Maeurer. 2003. Human papillomavirus type 16 E7 peptide-directed CD8$^+$ T cells from patients with cervical cancer are cross-reactive with the coronavirus NS2 protein. *J. Virol.* **77:** 5464–5474.
14. Orlando, V. 2003. Polycomb, epigenomes, and control of cell identity. *Cell* **112:** 599–606.
15. Rautajoki, K., T. A. Nyman, and R. Lahesmaa. 2004. Proteome characterization of human T helper 1 and 2 cells. *Proteomics* **4:** 84–92.
16. Riggs, D. L., P. J. Roberts, S. C. Chirillo, J. Cheung-Flynn, V. Prapapanich, T. Ratajczak, R. Gaber, D. Picard, and D. F. Smith. 2003. The Hsp90-binding peptidylprolyl isomerase FKBP52 potentiates glucocorticoid signaling *in vivo*. *EMBO J.* **22:** 1158–1167.
17. Rubin, B. Y., S. L. Anderson, L. Xing, R. J. Powell, and W. P. Tate. 1991. Interferon induces tryptophanyl-tRNA synthetase expression in human fibroblasts. *J. Biol. Chem.* **266:** 24245–24248.
18. Ruse, M., A. M. Broome, and R. L. Eckert. 2003. S100A7 (Psoriasin) interacts with epidermal fatty acid binding protein and localizes in focal adhesion-like structures in cultured keratinocytes. *J. Invest. Dermatol.* **121:** 132–141.
19. Salazar-Fontana, L. I. and B. E. Bierer. 2001. T-lymphocyte coactivator molecules. *Curr. Opin. Hematol.* **8:** 5–11.
20. Sansom, D. M. 2000. CD28, CTLA-4 and their ligands: Who does what and to whom? *Immunology* **101:** 169–177.
21. Satijn, D. P., D. J. Olson, J. van der Vlag, K. M. Hamer, C. Lambrechts, H. Masselink, M. J. Gunster, R. G. Sewalt, R. van Driel, and A. P. Otte. 1997. Interference with the expression of a novel human polycomb protein, hPc2, results in cellular transformation and apoptosis. *Mol. Cell. Biol.* **17:** 6076–6086.
22. Selin, L. K., M. Y. Lin, K. A. Kraemer, J. P. Schneck, D. Pardoll, S. M. Varga, P. A. Santolucito, A. K. Pinto, and R. M. Welsh. 1999. Attrition of T cell memory: Selective loss of LCMV epitope-specific memory CD8 T cells following infections with heterologous viruses. *Immunity* **11:** 733–742.
23. Selin, L. K., S. M. Varga, I. C. Wong, and R. M. Welsh. 1998. Protective heterologous antiviral immunity and enhanced immunopathogenesis mediated by memory T cell populations. *J. Exp. Med.* **188:** 1705–1715.
24. Sharpe, A. H. and G. J. Freeman. 2002. The B7-CD28 superfamily. *Nat. Rev. Immunol.* **2:** 116–126.
25. Tai, P. K., M. W. Albers, H. Chang, L. E. Faber, and S. L. Schreiber. 1992. Association of a 59 kDa immunophilin with the glucocorticoid receptor complex. *Science* **256:** 1315–1318.
26. Verdeil, G., D. Puthier, C. Nguyen, A.-M. Schmitt-Verhulst, and N. Auphan-Anezin. 2002. Gene profiling approach to establish the molecular bases for partial versus full activation of naïve CD8 T lymphocytes. *Ann. N.Y. Acad. Sci.* **975:** 68–76.

27. Vuadens, F., D. Gasparini, C. Deon, J.-C. Sanchez, D. F. Hochstrasser, P. Schneider, and J.-D. Tissot. 2001. Identification of specific proteins in different lymphocyte populations by proteomic tools. *Proteomics* **2:** 105–111.
28. Wadle, A., G. Thiel, A. Mischo, V. Jung, M. Pfreundschuh, and C. Renner. 2001. Chromosomal localization and promoter analysis of the adenomatous polyposis coli binding protein RP1. *Oncogene* **20:** 5920–5929.
29. Walsh, C. M., M. Matloubian, C. C. Liu, R. Ueda, C. G. Kurabara, J. L. Christensen, M. T. Huang, J. D. Young, R. Ahmed, and W. R. Clark. 1994. Immune function in mice lacking the perforin gene. *Proc. Natl. Acad. Sci. USA* **91:** 10854–10858.
30. Yan, J. X., R. Wait, T. Berkelman, R. A. Harry, J. A. Westbrook, C. H. Wheeler, and M. J. Dunn. 2000. A modified silver staining protocol for visualization of proteins compatible with matrix-assisted laser desorption/ionization and electrospray ionization-mass spectrometry. *Electrophoresis* **21:** 3666–3672.
31. Yim, S. B. and Y. H. Chung. 2004. Construction and production of concatameric human TNF receptor-immunoglobulin fusion proteins. *J. Microbiol. Biotechnol.* **14:** 81–89.
32. Zabazarnykh, M. Y. and D. Y. Litvinov. 2003. Phorbol ester stimulates expression of the human tryptophanyl-tRNA synthetase gene. *Biochemistry* (*Mosc*) **68:** 482–486.